Contents lists available at ScienceDirect

Physica B: Physics of Condensed Matter

journal homepage: www.elsevier.com/locate/physb

Effect of alkaline earth modifier on the optical and structural properties of Cu^{2+} doped phosphate glasses as a bandpass filter

M. Farouk [a,*], A. Samir [b], M. El Okr [a]

[a] Physics Department, Faculty of Science, Al- Azahr University, Nasr city, Cairo, 11884, Egypt
[b] Engineering Mathematics and Physics Department, Faculty of Engineering at Shoubra, Benha University, 11629, Egypt

ARTICLE INFO

ABSTRACT

Glasses of composition [16RO–3Al$_2$O$_3$—6CuO—20Na$_2$O—55P$_2$O$_5$], where R is the alkaline earth (R = Mg, Ca, Sr and Ba mol. %), were prepared by conventional melt quenching technique. The glass samples were characterized by X-ray diffraction, infrared spectroscopy, and spectrophotometer. XRD patterns show no sharp peaks indicating the non-crystalline nature of the prepared glasses. The density and molar volume of the glass systems were determined in order to study their structures. These results revealed that addition of alkaline earth elements leads to the formation of non-bridging oxygens (NBOs) and expands (opens up) the structure. The infrared spectra were analyzed to quantify the present phosphate groups. The optical absorption spectra of Cu^{2+} ions show the characteristic broadband single of Cu^{2+} ions in octahedral symmetry. The band gap was estimated following two methodologies. The first method considers the band edge of the transmission, while the second approach relays on the estimated values of the optical constants. A decent agreement for the band gap values using the two methods was obtained.

1. Introduction

Copper-doped phosphate glasses have interesting optical and electrical properties that make them suitable as color filters, solid state lasers, super-ionic conductors, and non-linear optics. The primary advantage of phosphate over other oxide glasses (e.g. silicate and borate) is their ability to accommodate high concentrations of transition metal ions and remain amorphous. In addition, phosphate glasses enjoy a range of compositional and structural possibilities (ultra, meta, pyro, and ortho) that facilitate tailoring chemical substance and physical behavior [1].

The poor chemical durability of phosphate glasses makes them generally unsuitable for practical applications. It was suggested that the chemical durability can be improved by the addition of one or more of multivalent oxides such as: Al$_2$O$_3$, SnO, ZnO,PbO, Fe$_2$O$_3$, etc., which promotes the formation of Al—O—P, Sn—O—P,Zn—O—P, Pb—O—P, Fe—O—P bonds, and subsequently increases the chemical durability to a measurable extent. A second alternative towards improving the chemical durability of phosphate glasses is the partial replacement of oxygen by nitrogen atoms [2–4]. In glasses, copper ions exist in more one valance state, monovalent (Cu$^+$) ions, and divalent (Cu^{2+}) ions and may also exist as metallic copper (Cu^0). The electronic structure of the copper atom is 3d^{10} 4s^1; the cuprous ion, having its 5 d orbitals occupied, does not produce coloring, while Cu^{2+} ions create color centers with an absorption band in the visible region and produce blue and green glasses. The color of the glass depends on the Cu^{2+} content, its specific coordination, composition and basicity of the glass. Colors produced by Cu^{2+} ions in various glasses have been interpreted in terms of ligand field theory [2,5–7]. Optical Filters are being used in many applications such as fluorescence microscopy, photography, optical device, spectroscopy, clinical chemistry, or machine vision inspection. Optical Filters are also suitable for life science, imaging and professional. Bandpass filters transmit a band of wavelengths spanning the region from 1 nm to hundreds of nanometers in width, while adjacent wavelengths are blocked. Band pass filters are, additionally, used in fluorescence microscopes to eliminate pump light from fluorescence signal light, eye protection from laser radiation by eliminating infrared laser light and passing only the visible light, and in sunglasses to pass the visible and block UV light [8].

2. Experimental details

The glassy system with composition [16RO–3Al$_2$O$_3$—6CuO—20Na$_2$O—55P$_2$O$_5$], where R is the alkaline earth elements (R = Mg, Ca, Sr and Ba mol %), were prepared by conventional melt quenching method. The starting materials used in the

---

* Corresponding author.
  E-mail address: mf_egypt22375@yahoo.com (M. Farouk).

present work were reagent grade of CuO, MgO, CaO, SrCO$_3$, BaCO$_3$, Na$_2$CO$_3$ and NH$_4$H$_2$PO$_4$. All weighted chemicals were powdered finally and were thoroughly mixed in an agate mortar. Each batch was introduced in porcelain crucibles in an electrical furnace at 400 ± 5 °C to remove water, ammonia and then melted at the 1100 ± 20 °C for 1.5 h. The melts were quenched between two brass plates to produce discs of about 0.2 cm thickness. The prepared samples were subjected to annealing at 350 ± 5 °C to remove internal stress. The glass samples obtained were homogeneous with green color. X-ray diffraction (XRD) spectra were obtained using a Shimadzu XD3A diffractometer. The densities of the prepared glass samples were measured by employing Archimedes's method with toluene as an immersion fluid (ρ = 1.595 kg/m^3). Infrared absorption spectra were recorded using FTIR (PerkinElmer) in the range (400-2000 cm^{-1}). The samples were prepared using the KBr disc technique. The absorption spectra were measured in the resolution of 1cm^{-1}. The optical absorption spectra of well-polished glass samples were taken at room temperature by UV–Vis spectrophotometer (JASCO V670) with the optical resolution 0.5 nm, in the wavelength range of 190–1100 nm.

3. Results and discussion

3.1. Physical parameters

The amorphous nature of the prepared glass samples was firstly examined by X-Ray diffraction (XRD) at room temperature. Fig. 1 displays the obtained XRD patterns which clearly do not present sharp diffraction peaks, confirming the non-crystalline characteristics of the prepared glasses.

Some properties of the investigated glass system are listed in Table 1. Fig. 2 hows the dependence of density and the molar volume (V$_M$) on the type of alkaline earth elements. The density of all glass samples increases by increasing the atomic weight of alkaline earth elements. This is most likely due to the fact that density is very sensitive to both the ionic size and atomic weight of the alkaline rare earth. Generally, it is always expected that the density and the molar volume should show opposite trend. However, in the present work, both the density and molar volume follow the same trend. Such an unusual behavior allows concluding that the addition of alkaline earth causes the formation of non-bridging oxygens (NBOs) and expands (opens up) the structure. This might also be due to change of metaborate network induced by the addition of alkaline earth.

The Cu-ion concentration (N) is the parameter of greatest interest as it affects different properties of the host material. The number of ions per cubic centimeter was calculated according to the following formula [9].
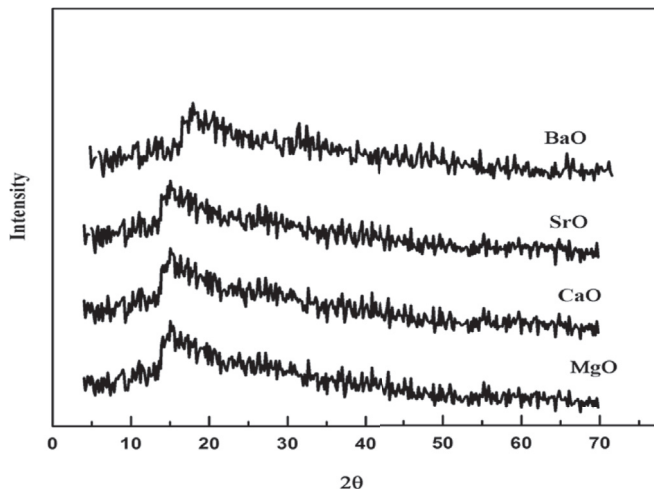
Table 1
Various physical parameters of Cu^{2+} doped sodium aluminum phosphate glasses.

Physical property	MgO	CaO	SrO	BaO
Density (g/cm^3) ±0.02	2.60	2.64	2.80	2.99
Average molecular weight (g)±0.02	104.72	107.25	114.85	122.81
Molar volume,V$_M$, (cm^3)±0.02	40.13	40.52	41.01	41.05
Cu^{2+}-ion concentration N (x10^{20} ions/cm^3)±0.02	8.99	8.91	8.80	8.79
Inter ionic distance (r_i) (x10^{-7}) cm ±0.0002	1.0357	1.0390	1.0433	1.0435
Field Strength F (x10^{15}cm^{-2})±0.0001	1.1482	1.1409	1.1317	1.1311

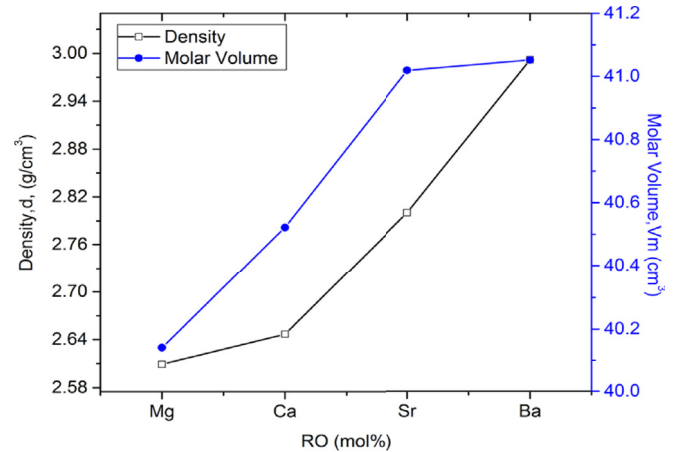**Fig. 2.** Dependence of density, and the molar volume, V$_M$, on alkaline earth elements.

$$N\left(\frac{ion}{cm^3}\right) = \frac{x\rho N_A}{M_w}$$

where N$_A$ is Avogadro's number, x is the mole fraction of the alkaline earth element, ρ is the density and M$_w$ is the average molecular weight of each sample. The calculated values of N are listed in Table 1 and plotted in Fig. 3. The data revealed that the Cu-ion concentration decreases, which is most likely due to the increase of Cu—Cu spacing. With the evaluated magnitudes of (N), it is possible to estimate three additional parameters [9]. These are;

$$r_p(A^o) = \left(\frac{1}{2}\right)\left(\frac{\pi}{6N}\right)^{1/3}$$
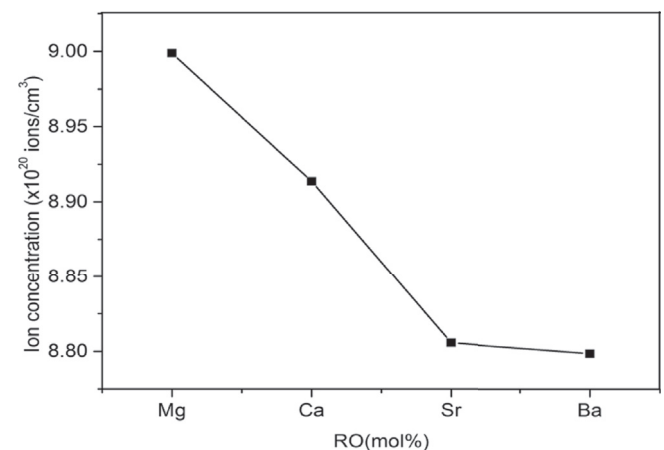
$$F\left(cm^2\right) = \frac{Z}{r_p^2}$$

Fig. 1. The X-ray diffraction patterns of the glass samples.

Fig. 3. Dependence of Cu^{2+}ion concentration, N, on alkali earth oxides.

$$r_i(A^o) = \left(\frac{1}{N}\right)^{\frac{1}{3}}$$

where r_p is the Polaron radius, F is the average field strength, Z is the valance of copper ion and r_i is the inter-ionic distance. The calculated values for each parameter are given in Table 1 and displayed in Fig. 4. It is generally assumed that the average ion separation and the field strength should follow an opposite trend, which is clearly observed in the present work. Furthermore, the average Cu ion separation increases, which can be attributed to the open structure caused by changing of the alkaline earth elements. The field strength (F) decreases with changing the alkaline earth elements, i.e., the results follow the common behavior, where the average Cu—Cu distance increases producing a weaker field around the Cu^{2+} ions. Therefore, changes in the physical properties of the prepared glasses are mainly due to the change in the host matrix around Cu^{2+} ions.

3.2. 3.2 FT-IR spectra

Infrared spectroscopy is usually used to get the essential information concerning the arrangement of the structural units of the studied glasses. It is assumed that vibrations of structural units in the glass network are independent of the vibrations of other neighboring units. The phosphate units in phosphate glasses exist in the range 1400–400 cm^{-1}. The infrared spectra of Cu^{2+} sodium aluminum phosphate glasses doped alkaline earth are shown in Fig. 5.

The spectral broadening is consistent with structures having various types of bonding. The obtained broad bands are a result of the overlap between some individual bands. Each individual band has its own characteristic parameters such as center, which is related to some type of vibrations of a specific structural group, and relative area, which is proportional to the concentration of these structural groups [10]. Fig. 6 shows the deconvoluted spectra assuming Gaussian bands. The deconvolution data (center position c, relative area A and the corresponding assigned vibrational modes) are given in Table 2. The band located at around 497-507 cm-1 is assigned to the bending vibrations of O—P—O linkages in the Q3 units [11]. The assignment of the band between 400 and 550 cm^{-1} is difficult because of the superposition of intermediates like MgO, CaO, SrO and BaO in the present glass system [12]. The band around 738–750 cm^{-1} is attributed to symmetric stretching vibrations of P—O—P rings in Q1 units [12]. The band near 881–978 cm^{-1} is due to the asymmetric stretching vibrations of the P—O—P linkage in Q2 units [13–15].

The observed strong band, in the region 800–1000 cm^{-1} in the spectra of all the investigated glasses, which is the characteristic of linear phosphates, suggests the presence of linear chains [12]. The band at
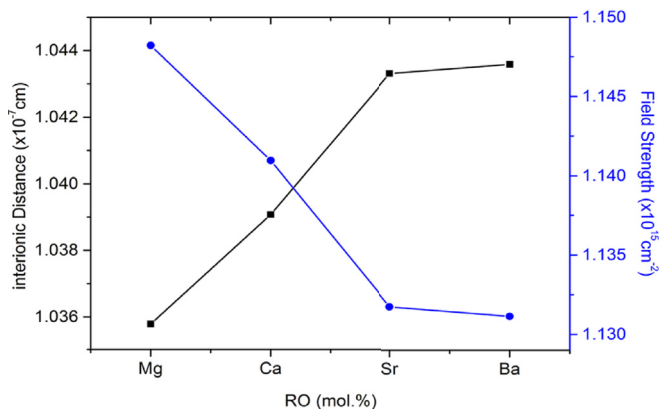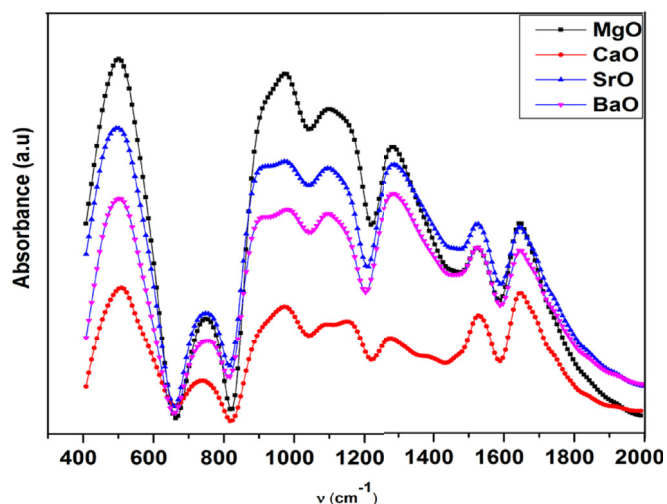

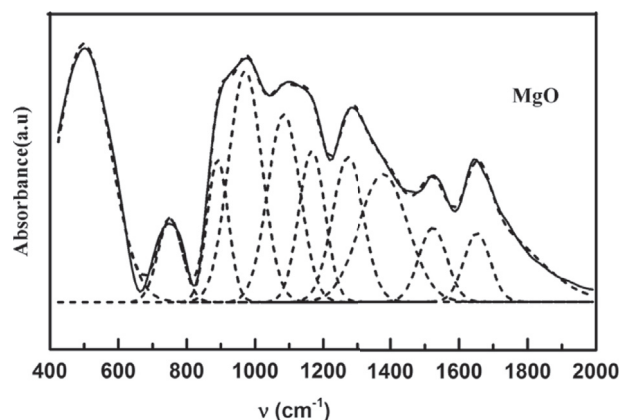Fig. 5. Infrared spectra of Cu^{2+} doped alkaline earth phosphate glasses.

Fig. 6. Deconvolution of IR spectra of MgO glass as example.

Table 2
Band assignments for IR spectra.

Band center c (cm^{-1})/Relative area A (± 3)				Band assignments
MgO	CaO	SrO	BaO	
497	507	496	501	O—P—O bending vibrations [13,14]
63	16	38	25	
750	738	747	747	P—O—P symmetric vibrations [13,14]
15.3	2	8.7	3.7	
881	891	891	885	P—O—P asymmetric stretching vibrations
15.1	2	3.5	6.3	[13,14].
977	966	978	975	(PO4) asymmetric stretching (Q0) [15].
34	8.9	35.7	20.7	
1102	1098	1112	1104	Symmetric stretching vibrations of Q2 (PO2)
25	9.3	9.6	13	groups [13,14]
1162	1169	1165	1161	PO2 − symmetric groups P͞O stretching
4	2.1	3.2	2.4	vibrations [16]
1267	1272	1270	1269	PO2 asymmetric groups P͞O stretching
25	6.1	11.8	11.5	vibrations [13,14]
1399	1417	1379	1376	Stretching modes of bridging oxygen in P͞O
28	8.2	26	24.9	bond [13]
1527	1530	1532	1532	bending vibrations H—O—H and P—OH in the
5	4.2	7	6.5	network (bridge) [7,15,18]
1656	1648	1644	1640	
12	4.1	5	3.2	

1098–1112 cm^{-1} is most likely due to the asymmetric stretching vibrations of $(PO3)^{2-}$ groups [15]. The band at 1161-1169 cm^{-1} is attributed

Fig. 4. Dependence of inter ionic distance, ri, and the field strength, F, on alkaline earth elements.

to the symmetric stretching vibrations of metaphosphate of PO2 groups [16]. The band around 1267–1270 cm^{-1} is associated with the asymmetric (P=O) stretching vibrations [13,14]. The band observed at 1376–1417 cm^{-1} has been attributed to symmetric stretching vibrations of bridging oxygen in P=O bond [13]. Introduction of modifiers, such as MgO, CaO, SrO and BaO, to the phosphate network would locate them among the non-bridging oxygens (NBOs), sharing corners with (PO4)$^{3-}$ groups that connect different phosphate chains such as P4O$_{13}^{6-}$, P3O$_{10}^{5-}$, and P2O$_7^{4-}$ [12,15]. The other two bands nearly at 1527–1532 cm^{-1} and 1644–1656 cm^{-1} are related to bending vibrations of O—H and P—OH bonds brought by air moisture during the preparation of KBr pellets for infrared measurements [10,11,15,17,18]. The changes in band position are not uniform as the alkaline rare earth changes. The shift to the lowest frequency is at calcium oxide (CaO).

3.3. Optical absorption studies

The UV transmittance is mostly influenced by heavier elements in the glass composition, melting technology and residual impurities. Heavy elements lead to increase in the refractive index and a decrease of transmittance in the UV region [19]. The transmission spectra of the glass samples in the wavelength range 190–1100 nm are shown in Fig. 7. As observed, aluminum phosphate glass containing Cu^{2+} ions and doped with alkaline earth, exhibit high optical transmission from about 350–650 nm. It is observed that sample containing SrO exhibits a higher transmittance while CaO has the lower transmission. One should expect that the addition of MgO, CaO, SrO and BrO causes fluctuations in the ligand field around the Cu^{2+} probe ion. This is related to changes in polarizability of oxygen ion surrounding the Cu^{2+} and its dependence on the field strength of the glass network [12]. The values of UV, IR cut off and UV bandstop are listed in Table 3.

The absorption spectra of the glass samples exhibit a broad absorption band around 780 nm and it is due to $^2B_{1g} \rightarrow {}^2B_{2g}$ octahedral transition of Cu^{2+} ions [19]. The Cu^{2+} ions is disturbed by an electronic hole in the degenerate orbital which has caused the tetragonal distortion according to Jahn-teller theory, i.e., any non-linear system with the degenerate ground state should distort in order to eliminate the degeneracy. Therefore, the structural changes may be possible, one is elongated and the other is compressed in the structure [12]. The band passes in optics are techniques that allow to pass a band of spectral lines through a filter [20,21]. The filter is characterized by parameters such as center c, FWHM, height and the area of the bandpass. Table 4 shows the change of these parameters with alkaline earth content (RO mol %). The center of the bands of Cu^{2+} doped glass samples shows that these filters lay in the green band.

3.3.1. Optical band gap energy (E_{opt}) and Urbach energy (ΔE)

The optical absorption is a convenient technique to understand the electronic structure in glasses. The dependence of the optical band gap on the composition of glasses gives information about the structure and the nature of bonds within the matrix. The absorption spectra of alkaline earth-aluminum phosphate glasses have been recorded in the wavelength range 190–1100 nm. All investigated glasses exhibit an optical absorption band in the UV, near infrared region and the fundamental optical absorption edge in the UV region. The absorption coefficient (α) of glass spectrum was calculated using the equation [22]:

$$\alpha(\nu) = \frac{1}{t} \log\left(\frac{I_0}{I}\right)$$

where t is the thickness of the sample and (I_0/I) corresponds to absorbance near the edge. $\alpha(\nu)$ can be related to optical band gaps for direct and indirect transitions following Davis and Mott [23]:

$$\alpha(\nu) = B\frac{\left(h\nu - E_{opt}\right)^n}{h\nu}$$

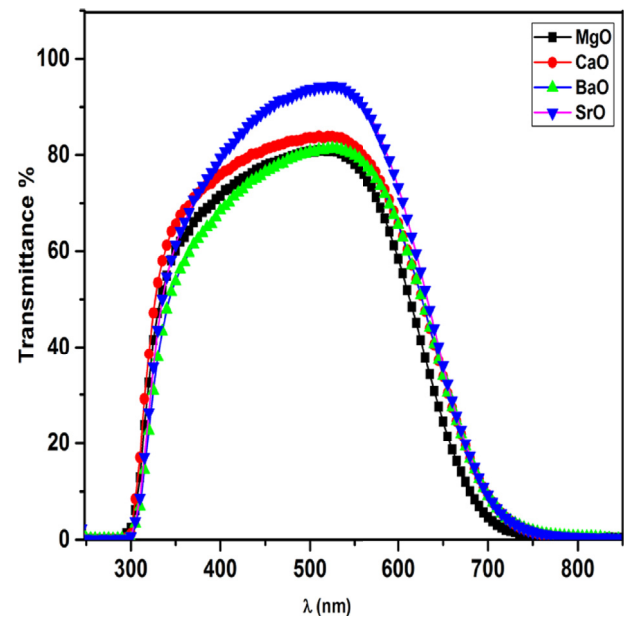**Fig. 7.** Optical transmission spectra of Cu^{2+} ions doped alkaline earth phosphate glasses.

Table 3
The optical parameters.

RO mol %	E_{opt} (ev) From ASF ±0.01	E_{opt} (ev) From ε_2 ±0.01	E_e (ev) ±0.003	UV cut off ±3	UV Bandstop ±4	IR cut off ±3
MgO	3.64	3.65	0.293	293	190–293	771
CaO	3.68	3.78	0.287	290	190–290	796
SrO	3.56	3.68	0.295	294	190–294	820
BaO	3.52	3.62	0.299	295	190–295	815

Table 4
The center (C), area (A), full width at half maximum (FWHM) and height of bandpass filter.

RO mol%	C (nm)	A (cm^2)	FWHM	Height
MgO	482.2	25563.8	263.8	81
CaO	485.6	28146.8	277.7	84
SrO	498.6	29084	274	94
BaO	499.9	25707.7	278.2	81.04

where B is a constant, E_{opt} is the optical band gap energy, and n may have the following values 2, 3, 1/2 and 1/3 depending on the interband electronic transition (direct and indirect). The analysis of the data reveal that in the present case n = 2, indicating an indirect transition. From the plots of $(\alpha h\nu)1/2$ as a function of photon energy ($h\nu$), the values of E_{opt} can be obtained by the extrapolation of the linear region of the plots to the $h\nu$ axis for indirect transitions and are shown in Fig. 8.

The width of the tail of the absorption spectra can also be used to analyze possible changes in the glass structure [23]. It is worth noted that for lower values of the absorption coefficient $\alpha(\nu) \approx 103$–104 cm^{-1}, it exhibits an exponential increase and is given by Refs. [24,25]:

$$\alpha(\nu) = \alpha_0 \exp\left(\frac{h\nu}{\Delta E}\right)$$

where α_0 is a constant, $h\nu$ is the photon energy and ΔE is the Urbach energy, which indicates the width of the band tail of the localized states in the band gap. The Urbach energy (ΔE) values of the present glass samples were determined by taking the reciprocals of the slopes of the linear part of the ln(α) versus $h\nu$ plots as shown in Fig. 9.

The obtained values of E_{opt} and ΔE are listed in Table 3 and plotted in
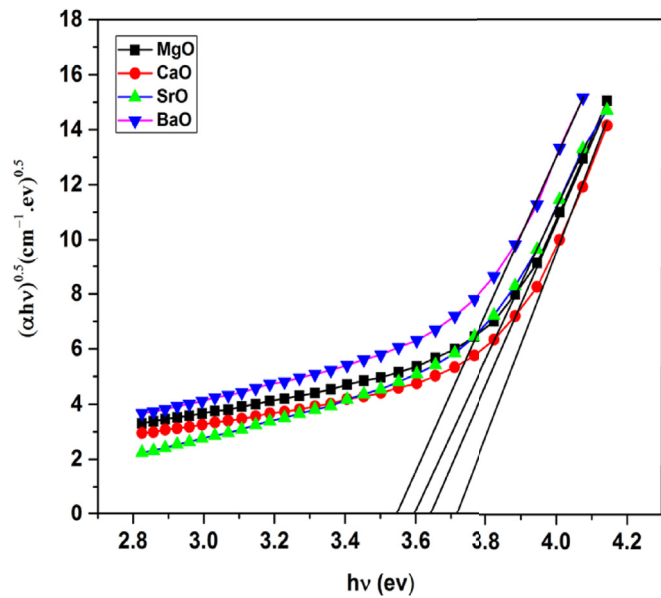
Fig. 8. Tauc's plot for Cu^{2+} ions doped alkaline earth phosphate glasses.

Fig. 10. Dependence of optical band gap (E_{opt}) and the Urbach's Energy (ΔE) with the content of alkaline earth.

Fig. 11. Imaginary part of the dielectric constant as a function of photon energy.

Fig. 10. It is clear that they follow opposite trends. The values of the optical band gap vary with the alkaline earth oxide content. The E_{opt} values of these glasses are in the same range observed for another glassy system [12]. In fact, alkaline earth additives may enhance the degree of localization by creating defects. The addition of network modifiers, such as alkaline earth oxides, breaks these bridges and creates non-bridging oxygens (NBOs). The increase in E_{opt} for the glass samples could be related to the increase of the cross-linking density in the glassy matrix [25]. Urbach energy values decrease with increasing the alkaline earth contents. The obtained smaller values of Urbach energy indicates that Cu^{2+} doped alkaline earth-aluminum phosphate glasses are homogeneous and stable [12]. This is likely to be related to the increase in the number of NBOs in the glass matrix, which means enhancement of the degree of disorder that causes more defects or localized states in the band gap [25,26].

Optical energy gaps (E_{opt}) were also calculated using the imaginary part of the dielectric constant, ε_2. Imaginary and real parts of dielectric constant (ε_2; ε_1) are calculated by using the relations [27,28]:

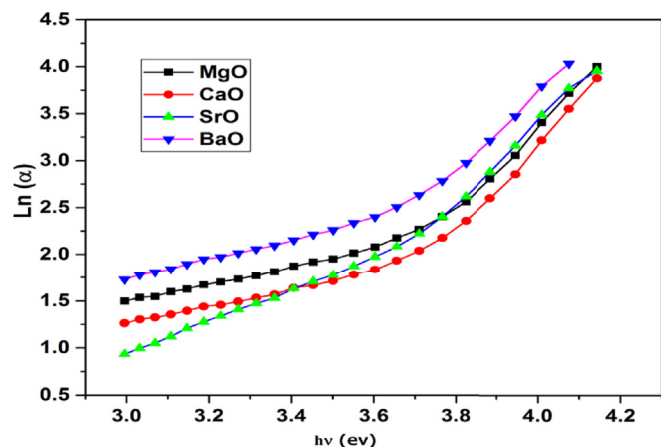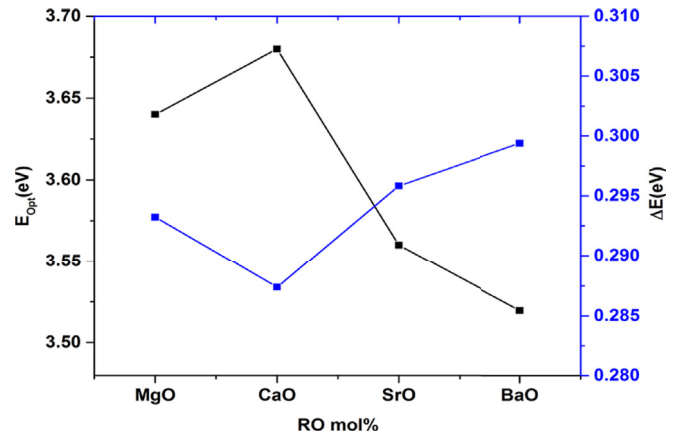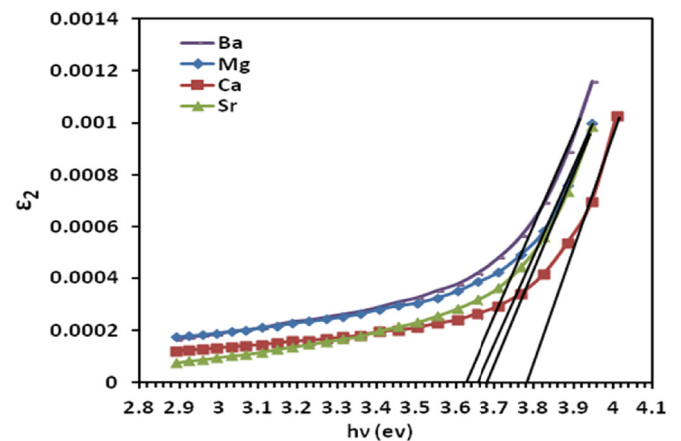$$n^2 = \frac{1 + R^{\frac{1}{2}}}{1 - R^{\frac{1}{2}}}$$

$$K = \alpha\lambda / 4\pi$$

$$\varepsilon_1 = n^2 - k^2$$

$$\varepsilon_2 = 2nk$$

where n is the refractive index, k is extinction coefficient and α is

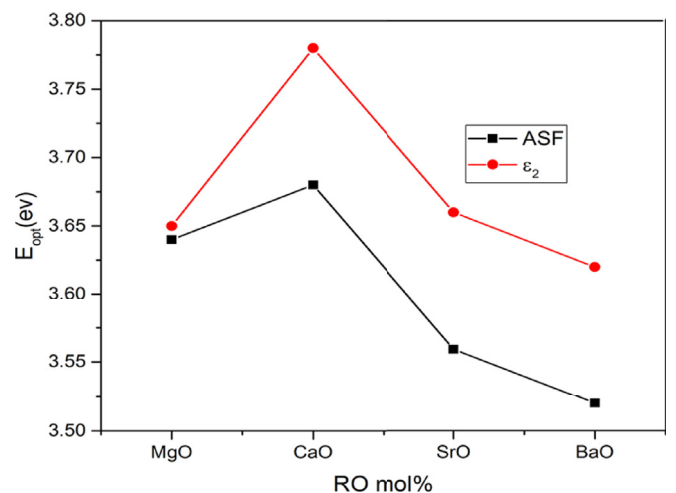**Fig. 9.** Urbach plot for Cu^{2+} ions doped alkaline earth phosphate glasses.

Fig. 12. Comparison of band gap energy values which calculated from the absorption spectrum fitting (ASF) method and imaginary part of the dielectric constant (ε_2) as a function of alkaline earth.

absorption coefficient. The variation of imaginary part of the dielectric constant (ε_2), with the photon energy (hν), is shown in Fig. 11. The optical band gap (E_{opt}) can be obtained by extrapolating the imaginary part of the dielectric constant ($\varepsilon 2$) to zero. Fig. 12 shows the comparison of band gap energy values calculated from the absorption spectrum fitting (ASF) method and from the imaginary part of the dielectric constant (ε_2). The energy gap values obtained from both methods are in agreement with each other as depicted in Table 3.

4. Conclusion

The glass systems of composition [16RO–3Al$_2$O$_3$—6CuO—20Na$_2$O—55P$_2$O$_5$], (R = Mg, Ca, Sr and Ba mol.%), were prepared and the effect of alkaline earth on the structure and properties of phosphate glass doped CuO was investigated. The results of XRD show that all glasses are amorphous. The behavior of density and molar volume allows to conclude that alkaline earth elements additives lead to the formation of non-bridging oxygens (NBOs) and expand (opens up) the structure. The infrared spectra were analyzed to quantify the present phosphate groups. The changes in band position were not uniform as the alkaline rare earth changes. The filter was characterized by the parameters such as center c, FWHM, height and the area of the bandpass. The band gap energy values were calculated from the absorption spectrum fitting (ASF) method and imaginary part of the dielectric constant (ε_2). The energy gap values obtained from both methods are in agreement with each other.

References

[1] E. Metwalli, M. Karabulut, D.L. Sidebottom, M.M. Morsi, R.K. Brow, J. Non-Cryst. Solids 344 (2004) 128.

[2] L. Srinivasa Rao, M. Srinivasa Reddy, D. Krishna Rao, N. Veeraiah, Solid State Sci. 11 (2009) 578.

[3] A. Chahine, M. Et-Tabirou, M. Elbenaissi, M. Haddadb, J.L. Pascal, Mater. Chem. Phys. 84 (2004) 341.

[4] P.Y. Shiha, T.S. Chin, Mater. Chem. Phys. 60 (1999) 50.

[5] Byeng-soo Bae, Michel C. Weinbergi, J. Non-Cryst. Solids 168 (1994) 223.

[6] M.V. Sambasiva Rao, S. Suresh, T. Narendrudu, A. Suneel Kumar, G. Chinna Ram, D. Krishna Rao, J. Mol. Struct. 1125 (2016) 624.

[7] T. Wongsing, J. Kaewkhaob, P. Limsuwana, C. Kedkaewa, Proc. Eng. 32 (2012) 807.

[8] Vijay Laxmi Kalyani, Varsha Sharma, JMEIT 3 (2016) 2394.

[9] A.S. Rao, Y.N. Ahammed, R.R. Reddy, T.V.R. Rao, Opt. Mater 10 (1998) 245.

[10] Y. Lai, X. Liang, G. Yin, S. Yang, J. Wang, H. Zhu, H. Yu, J. Mol. Struct. 1004 (2011) 188.

[11] Y.B. Saddeek, Phys. B 406 (2011) 562.

[12] S. Sreehari Sastry, B. Rupa Venkateswara Rao, Phys. B 434 (2014) 159.

[13] P. Kumar Jha, O.P. Pandey, K. Singh, J. Mol. Struct. 1094 (2015) 174.

[14] A. Suneel Kumar, T. Narendrudu, S. Suresh, M.V. Sambasiva Rao, G. Chinna Ram, D. Krishna Rao, J. Non-Cryst. Solids 434 (2016) 62.

[15] S. Li, H. Liua, Y. Lu, Y. Qu, Y. Yue, J. Non-Cryst. Solids 450 (2016) 87.

[16] M. Atef Cherbib, S. Krimi, A. El Jazouli, I. Khattech, L. Montagne, B. Revel, M. Jemal, J. Non-Cryst. Solids 447 (2016) 59.

[17] Y.C. Ratnakaram, S. Babu, L. Krishna Bharat, C. Nayak, J. Lumin 75 (2016) 57.

[18] Y.M. Lai, X.F. Liang, S.Y. Yang, J.X. Wang, L.H. Cao, B. Dai, J. Mol. Struct. 992 (2011) 84.

[19] Ch Tirupataiah, T. Narendrudu, S. Suresh, P. Srinivasa Rao, P.M. Vinaya Teja, M.V. Sambasiva Rao, G. Chinna Ram, D. Krishna Rao, Opt. Mater 73 (2017) 7.

[20] H. Elhaes, M. Attallah, Y. Elbashar, M. El-Okr, M. Ibrahim, Phys. B 449 (2014) 251.

[21] Y. H. Elbashar, Silicon, DOI 10.1007/s12633-016-9429-5.

[22] M. Farouk, A. Abd El-Maboud, M. Ibrahim, A. Ratep, I. Kashif, Spectrochim. Acta. Part A 149 (2015) 338.

[23] N.F. Mott, E.A. Davis, Philos. Mag. 17 (1968) 1269.

[24] F. Urbach, Phys. Rev. 92 (1953) 1324.

[25] I. Jlassi, H. Elhouichet, M. Ferid, Phys. B 81 (2016) 219.

[26] Ch Rajyasree, A. Ramesh Babu, D. Krishna Rao, J. Mol. Struct. 1033 (2013) 200.

[27] Shaik Ahmmad, M.A. Samee, A. Edukondalu, S. Rahman, Results Phys. 2 (2012) 175.

[28] G. Samdani, M. Ramadevudu, Narasimha Chary, Md Shareefuddin, Mater. Chem. Phys. 186 (2017) 382.